ISSN No: 2348-4845
International Journal & Magazine of Engineering, Technology, Management and Research
A Peer Reviewed Open Access International Journal

Modeling of Tool Influence Function for High Efficiency Polishing Compared With Ansys

Bylapudi Srinu
Department of Machanical Engineering,
Chaitanya Engineering College,
Visakhapatnam, Andhra Pradesh – 530041, India.

P.Santhi
Department of Machanical Engineering,
Chaitanya Engineering College,
Visakhapatnam, Andhra Pradesh – 530041, India.

ABSTRACT:

The M-shaped tool influence function (TIF) usually comes out when adopting a large tool offset at the high efficiency polishing stage in bonnet polishing. Its modeling is as important as the Gaussian-like TIF for the polishing process. Computer controlled polishing requires accurate knowledge of the tool influence function (TIF) for the polishing tool (i.e. lap). While a linear Preston's model for material removal allows the TIF to be determined for most cases, nonlinear removal behavior as the tool runs over the edge of the part introduces a difficulty in modeling the edge TIF. We provide a new parametric model that fits 5 parameters to measured data to accurately predict the edge TIF for cases of a polishing tool that is either spinning or orbiting over the edge of the work piece. However, the existing reports on the TIF of bonnet polishing are mostly about the Gaussian-like TIF model, or the model which cannot accurately simulate the M-shaped TIF. Viewing this, an optimized TIF model about the semi rigid (SR) bonnet tool is presented based on the finite element analysis method which can be used to model M-shaped and Gaussian-like TIFs. The verification experiments show that the simulated TIFs based on this model are in good agreement with the actual measured TIF. Pressure distribution in the contact area is confirmed based on finite element analysis (FEA) technology and Analytical method is compared.

INTRODUCTION:

Tool influence function is the basic stage of tool path generation and is often considered as an image of contact impression of the tool.

The various parameters that define the characteristics of TIF are to be analysed due to its strict correlation with product: on-time delivery delay, surface defects, competitive market advantage etc. Different tools have been developed in the past in the area of research with unique TIF profiles based on the requirement. The dwell time of the tool on a work surface is determined by the tool influence function. Smoother volume of TIF combined with an optimum selection of step over distance can significantly reduce the value of peak to valley depth, an indicator of error to removal factor [1]. Precision optical surfaces, such as plane, spherical, even aspheric or freeform surfaces, have always been a challenge. And the requirement for optical elements have steadily increased, concerning surface figure, surfaces/sub-surface quality, deviation of RMS of irregularity, mid-spatial-frequency and power spectrum density. Conventional polishing is done mainly by skilful workers using specialized tools, which is not feasible for precision products. Since computer controlled polishing (CCP) processes were developed in the 1960s, there have been a number of emerging technologies that are enabling the cost-effective manufacture of precision surfaces, particularly sub aperture polishing. Sub aperture polishing technologies have radically changed the landscape of precision optics manufacturing and enabled the production of components with higher accuracies and increasingly difficult figure requirements, including ion beam figuring,

Cite this article as: Bylapudi Srinu & P.Santhi, "Modeling of Tool Influence Function for High Efficiency Polishing Compared With Ansys", International Journal & Magazine of Engineering, Technology, Management and Research, Volume 5, Issue 4, 2018, Page 1-10.

ISSN No: 2348-4845
International Journal & Magazine of Engineering, Technology, Management and Research
A Peer Reviewed Open Access International Journal

plasma-assisted chemical etching, magneto rheological finishing, magneto rheological jet polishing, even a fiber-based tool polishing. Although these processes have radically different polishing mechanisms, many large aspheric even off-axis segments have been successfully fabricated using them [2]. A novel approach, the precessions polishing process, proposed by D.D. Walker group, was a type of sub-aperture technology. A tool is comprised of an inflated, bulged rubber membrane of spherical form (bonnet), and covered with standard flexible polishing cloths. The standard polishing slurries was used in this process. Precession motion was induced to produce a mathematically well behaved near-Gaussian influence function. The bonnet polisher rocked about its pole through precise CNC control of the position and orientation of a spinning. Recently, the process was successfully applied to control the edge zoom of hexagonal segments fabrication [3]. The demand for an efficient work piece edge figuring process have been increased due to the popularity of segmented optics in many next generation optical systems, such as the Giant Magellan Telescope (GMT) and James Webb Space Telescope (JWST) .

Because those systems have multiple mirror segments as their primary or secondary mirrors, i) the total length of edges is much larger than the conventional system with one mirror; ii) the edges are distributed across the whole pupil. Thus, a precise and efficient edge fabrication method is important to ensure the final performance of the optical system (e.g. light collecting power and spatial resolution based on the point spread function) and reasonable delivery time [5]. Many Computer Controlled Optical Surfacing (CCOS) techniques have been presented and developed since 1972 . The CCOS with its superb ability to control material removal is known as an ideal method to fabricate state-of-the-art optical surfaces, such as meter-class optics, segmented mirrors, off-axis mirrors, and so forth. The dwell time map of a tool on the work piece is usually the primary control parameter to achieve a target removal (i.e. form error on the work piece) as it can be modulated via altering the transverse speed of the tool on the work piece .In order to calculate an optimized dwell time map, the CCOS mainly relies on a de-convolution process of the target removal using a Tool Influence Function (TIF) (i.e. the material removal map for a given tool and work piece motion) [4]. Thus, one of the most important elements for a successful CCOS is to obtain an accurate TIF.

1.1 POLISHING:

Polishing is the process of creating a smooth and shiny surface by rubbing it or using a chemical action, leaving a surface with a significant specular reflection (still limited by the index of refraction of the material according to the Fresnel equations.)In some materials (such as metals, glasses, black or transparent stones), polishing is also able to reduce diffuse reflection to minimal values. When an unpolished surface is magnified thousands of times, it usually looks like mountains and valleys. By repeated abrasion, those "mountains" are worn down until they are flat or just small "hills." The process of polishing with abrasives starts with coarse ones and graduates to fine ones. The strength of polished products is normally higher than their rougher counterpart owing to the removal of stress concentrations present in the rough surface. They take the form of corners and other defects which magnify the local stress beyond the inherent strength of the material [6]. Polishing with very fine abrasive differs physically from coarser abrasion, in that material is removed on a molecular level, so that the rate is correlated to the boiling point rather than to the melting point of the material being polished.

1.2 TOOL INFLUENCE FUNCTION:

The tool influence function (TIF) serves as an important and indispensable variable in the optical surfacing system. It represents the material removal produced by a polishing tool in a unit of time. In the practical polishing process, the TIF would be taken into the calculation of dwell time.

ISSN No: 2348-4845
International Journal & Magazine of Engineering, Technology, Management and Research
A Peer Reviewed Open Access International Journal

Its peak removal rate (PRR) and shape would generate a huge influence on the magnitude and distribution of the dwell-time map. Based on the Preston function, the theoretical model of TIFs can be built through the corresponding motion model and pressure distribution model. According to the Fourier transform theory, we can conclude two important equations:

$$\widetilde{TIF} = \oint_{-\infty}^{\infty} TIF(x,y)dxdy \quad (1)$$

$$TIF = \oint_{-\infty}^{\infty} \widetilde{TIF}(\varepsilon,\eta)d\varepsilon d\eta \quad (2)$$

Equation (1) indicates that the direct current (DC) response of polishing systems is constructed by the integration of TIF in the space domain. The integration value is always non-negative because of the non-negativity of TIFs. We can obtain uniform material on the surface if uniform polishing is conducted on the surface. Equation (2) illustrates that a TIF with zero central removal can remove a certain period of surface errors but leave more mid–high spatial frequency errors. If the TIF has central peak removal, the surface error can be convergent one-by-one with increasing polishing times. Thus, from the above analysis, the basic characteristics of TIFs can be concluded as:

- A TIF should be a rotational-symmetric and smooth function.
- A TIF has central peak removal and decreases as the radius increases.
- A TIF has no material removal when the distance exceeds the maximum radius.
- The slope of a TIF at the center and edge regions should be zero.

Since the 1970s, people have taken more than 40 years to find an ideal polishing tool with perfect TIFs. New tools with different work principles emerge every few years. Their purpose is only to improve the performance of material removal on removal rate, roughness, free-edge effect, non-subsurface damage, and stability. Removal rate directly affects the fabrication efficiency, which is referred to as the primary purpose to some extent.

The roughness performance is also significant; it influences the distribution of high-spatial frequency errors, which has strict demands in x-ray and laser gyroscope systems. The ideal polishing tool should also have no subsurface damage to ensure that no damage exists on the subsurface of optical segments, as this damage would diminish the long-term stability of optical systems and the coating quality, image performance, and laser-induced damage threshold of optical elements. Contact-type polishing tools remove material by relying on contact pressure, which results in an edge effect when the tool dwells in the edge region of the segment. Stability also serves as an indispensable target, as the convergence rate of surface form would largely decrease if the stability of the TIF is low. The ideal TIF should always remain invariant during the entire fabrication.

Cutoff Frequency for Removal Capability

The removal capability of a TIF for localized residual errors has great significance for high fabrication accuracy of optical surfaces. From this view, the best TIF should be a pulsing function that which could correct any localized residual errors. However, we could not obtain a pulsing TIF in any case. If a TIF performs closer to a pulsing function, it has much higher removal capability for localized residual errors. For a certain size TIF, the shape has a large influence on the removal capability. From the frequency domain, the normalized amplitude frequency spectrum of a TIF can be expressed as:

$$TIF_F(w) = FFT(TIF_n(r)) \quad (6)$$

Where FFT represents Fast Fourier Transform, and $TIF_n(r)$ represents the normalized TIF. An example of a normalized amplitude frequency spectrum curve is shown in Fig. 2.1. Figure 1a displays a typical TIF. Figure 2.1b is the corresponding normalized amplitude frequency spectrum curve, which quickly drops down to near-zero. For a specific spatial frequency, a higher normalized amplitude represents a higher removal capability for localized small errors.

ISSN No: 2348-4845
International Journal & Magazine of Engineering, Technology, Management and Research
A Peer Reviewed Open Access International Journal

The cutoff frequency represents the specific spatial frequency where the normalized amplitude spectrum curve reduces to 0.05 (point A shown in Fig.1b); we consider that the TIF could not generate a valid correction for the localized error whose spatial frequency exceeds the cutoff frequency. For a TIF with a certain size, the cutoff frequency could evaluate the removal capability for localized errors. A higher cutoff frequency means higher removal capability for localized small errors.

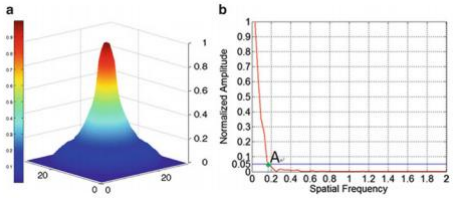

Fig1.1 (a) The typical TIF; (b)

1.3 The removal function:

The tool removal function depends on the relative velocity and pressure distribution mainly, and other conditions which was considered as the process dependent coefficient. There are three working modes based on processing attitude, plumb processing mode, tilt processing mode, and precession processing mode. Actually for plumb processing mode, the material removal of the centre of polishing spot is zero, and the profile of the tool function looks like V shape. It is not commonly used for fabrication.

2. LITERATURE REVIEW:

C. Wang et al. [1] studied the effect of different tools on bonnet polishing. They developed a technique to mathematically model a set of three different static tool influence functions: TIF of tilted polishing, TIF of discrete precision polishing and TIF of continuous precision polishing. The purpose of this work was to analyse the effect of pressure distribution & velocity on the depth of removal and possible substitutions of the generated functions. In their approach, FEA was used to understand the effect of pressure distribution on the material and the spots for the polishing operation was extracted from a set of data through experiments.

DaeWook Kim et al. [2] have also explained the difference between conventional optimization and non-sequential optimization. In conventional optimization, optimization engine searches for the best and suitable optimal dwell time value for a TIF on the work piece which can give the best residual error map. On the contrary, non–sequential optimization uses various TIF's in a single optimization. Each TIF has its own dwell time map and the removal is calculated by a combination of different TIF and its own dwell time map. The key difference between them is to find the optimal dwell time map solution. Gradient descent method is the most simple and straight forward optimization technique because it moves to the next point by minimizing a figure of merit. The two general weaknesses of this technique are as follows It may take many iterations to arrive the optimal solution in the search space Improper perturbation step to calculate the local gradient may result in poor optimization performance. In non-sequential optimization technique, mid-spatial frequency error is identified and rectified by comparing the different cases for the optimization technique

Hongyu Li et al. [3] studied the edge polishing of hexagonal part with the development of precession process. The purpose of the paper was to analyse and overcome problems while the polishing part is overhung at a significant length. With the help of tool-lift method, the bonnet tool is progressively raised or lowered (z offset), delivering polishing spot (Tool influence function or TIFs) of variable size. It also enables the spots to be controlled so that overlapping of the edge is overcome. Edge TIF can be simulated in two ways: modelling the surface speed distribution across the TIF and using the pressure distribution method at the edge of the part by FEA.

ISSN No: 2348-4845
International Journal & Magazine of Engineering, Technology, Management and Research
A Peer Reviewed Open Access International Journal

3. THEORETICAL BACKGROUND

Mathematical model of polishing process with bonnet polisher

The TIF can be calculated based on the equation of material removal, Δz, which is known as the Preston's equation

$$\Delta Z(x, y) = K \cdot P(x, y) \cdot VT(x, y) \cdot \Delta t(x, y) \quad (1)$$

Where Δz denotes the material removal depth; κ is the process-dependent coefficient related to the work piece material, polishing-tool, polishing slurry and temperature of work environment, etc. P(x, y) and V(x, y) are the pressure and the relative velocity distribution between tool and optic, respectively; Δt is the working time of the tool staying on the optic.

3.2. The tool function of bonnet polisher:

The tool function of bonnet polisher can be determined through the velocity and the pressure distribution on given working condition based on Preston Equation. During polishing, the bonnet polisher with spherical form was numerically controlled downward to work piece with h distance (compression values) from the position the polisher just contact with the work piece. Then, the tool polisher rotated around its axis, and the rotation axis rocked around the normal of the surface being polished. Figure 1 shows the diagram of the movement of bonnet polisher. Where Sarea is the contacted circle area between tool and work piece, O is the centre of Sarea, R is the radius of bonnet polisher; Line MN is the rotation axis of bonnet, and the rotation speed is ω0; the bonnet polisher also rotates about the Z-axis with ω1; θ is the so-called precession angle between two axes.

3.3. Linear pressure distribution model:

Assuming the linear pressure distribution and Preston's relation, we determine the resulting TIF analytically. Assume local coordinate system, (x, y), centered at the work piece edge with the x axis in the overhang direction (i.e. the radial direction from the work piece center).

The pressure distribution under the tool-work piece contact area should satisfy two conditions.

i) The total force, f0, applied on the tool should be the same as the integral of the pressure distribution, p(x, y), over the tool-work piece contact area, A. ii) The total sum of the moment on the tool should be zero. It is assumed that the pressure distribution in y direction is constant, and it is symmetric with respect to the x axis. The moment needs to be calculated about the center of mass of the tool, (x', y'). These two conditions are expressed in Eqs. (2) and (3), respectively

$$\iint_A p\,(x, y)\,dxdy = f_0 \quad (2)$$

$$\iint_A (x - x').\,p(x - x', y)\,dxdy = 0 \quad (3)$$

Where x is the x coordinate of the center of mass of the tool. While we acknowledge the freedom of choosing virtually any form of mathematical function for the analytical expression of pressure distribution, R.A. Jones introduced the linear pressure distribution model, Eq. (4), in 1986 on the tool-work piece contact area without detailed study of many higher order factors such as tool bending.

$$p\,(x, y) = C_1.x + C_2 \quad (4)$$

The pressure distribution, p(x, y), is determined by solving two equations, Eqs. (2) and (3), for two unknown coefficients, c1 and c2. Even though this analytical solution yields negative pressures for large overhang cases, we can replace it with zero pressure in practice and solve for c1 and c2 by iteration. Some examples of the linear pressure distribution, p(x), are plotted in Fig. 1 (left) when a circular tool overhang ratio, Stool, changes from 0 to 0.3. Stool is defined as the ratio of the overhang distance, H, to the tool width in the overhang direction, W_{tool}, in Fig.1(left).This linear pressure model was fed into the Preston's equation, Eq. (1), to generate the basic edge TIF in Section 3.1

ISSN No: 2348-4845
International Journal & Magazine of Engineering, Technology, Management and Research
A Peer Reviewed Open Access International Journal

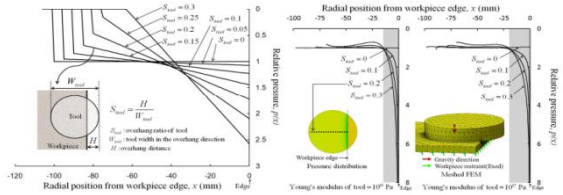

Fig 3.1: x- profiles of the pressure distribution, p(x, y), under the tool-work piece contact area: linear pressure distribution model. (Left), static FEA results. (Right).

3.4. Relative velocity distribution:

In this work, the relative velocity distribution can be obtained according to the geometrical relationship of the tool-motion. The velocity relation of any point (Q) in the polishing contact zone includes linear velocity vector $\vec{V}_0$and $\vec{V}_1$ · $\vec{V}_0$ is the linear velocity vector rotating about MN axis, and $\vec{V}_1$is the linear velocity vector rotating about Z-axis. In Figure 1, point N is in XOY plain with polar angle α, QD is the distance between point Q and rotate axis MN, QA is the distance between point Q and ON. From known conditions, the coordination of point M is (0, 0, R h), and the coordination of point N is

$$\begin{cases} N_x = (R-h)\tan\theta\cos x \\ N_y = (R-h)\tan\theta\sin x \\ N_z = 0 \end{cases}$$

Then |OE| = r ·cos (α +π − φ), |ON| = (R -h) tanθ. Suppose the polar angle of point Q(x, y) is φ (0 ≤ φ ≤ 2 π), and tan φ = y/x, r =$\sqrt{x^2+y^2}$, the coordination of point A is

$$\begin{cases} A_x = r\cos(\varphi-\alpha)\cos\alpha \\ A_y = r\cos(\varphi-\alpha)\sin\alpha \\ A_z = 0 \end{cases}$$

The coordination of point D is

$$\begin{cases} D_x = (\,(|\overrightarrow{ON}| - |\overrightarrow{OA}|)\cos^2\theta + |\overrightarrow{OA}|)\cos\alpha \\ D_y = (\,(|\overrightarrow{ON}| - |\overrightarrow{OA}|)\cos^2\theta + |\overrightarrow{OA}|)\sin\alpha \\ D_z = (\,(|\overrightarrow{ON}| - |\overrightarrow{OA}|)\cos\theta\sin\theta \end{cases}$$

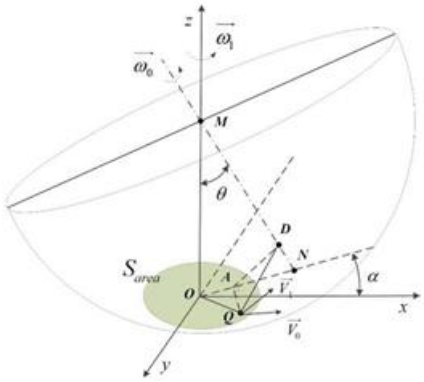

Fig 3.2: Diagram of movement of bonnet polisher, the dashed line

At last, the linear velocity $\vec{V}_0$ and $\vec{V}_1$ can be obtained, respectively,

$$\vec{V}_0 = \frac{\overrightarrow{NM}\times\overrightarrow{DQ}}{|\overrightarrow{NM}|}\vec{\omega}_0$$

$$\vec{V}_1 = \frac{\overrightarrow{OM}\times\overrightarrow{OQ}}{|\overrightarrow{OM}|}\vec{\omega}_1$$

Where $\overrightarrow{NM}$= M – N, $\overrightarrow{DQ}$ = Q – D, $\overrightarrow{OQ}$ = Q – O ,$|\overrightarrow{NM}|$ and $|\overrightarrow{OM}|$are the magnitude of $|\overrightarrow{NM}|$ and $|\overrightarrow{OM}|$respectively. The velocity vector of point Q, a space vector changing with its coordination (point Q), is $\vec{V}$ = $\vec{V}_0$+ $\vec{V}_1$. Because the motion of point Q was constrained in contacted area, normally its projection in the x-y plane was used during calculation. The relative velocity of Q can be expressed by below Equation. Then the relative velocity distribution can be calculated by traversing all point in contact zone.

$$|V_Q| = \sqrt{V_x{}^2 + V_y{}^2}$$

where$V_x$and$V_y$are the components of the vector ($\vec{V}$). The nonzero component $V_z$may cause an extra pressure, (for plane surface, it will be zero). Generally the contact zone is small, it can be approximately considered to be planar. And, component $V_z$is very small. In this work, we neglect the extra pressure due to nonzero component V_z.

ISSN No: 2348-4845
International Journal & Magazine of Engineering, Technology, Management and Research
A Peer Reviewed Open Access International Journal

4. MODELLING:

The initial bonnet tool has a spherical shape. Under the effect of the inner pressure , the bonnet contour deformed to aspheric shape shown in the below figure. Also , if the tool contour is spherical, the shape of the contact spot would be a standard circle.But due to the effect of tool deformation, the contact spot shape becomes irregular.

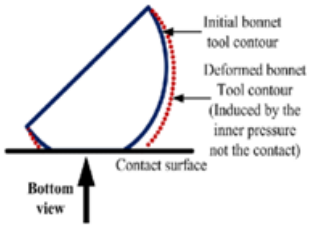

Fig 4.1 : bottom view

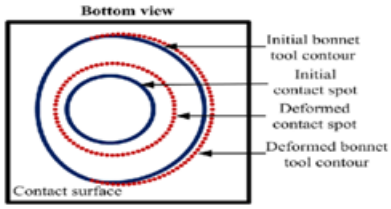

Fig 4.2: bottom view

Table 4: Properties

Tool size (mm)	Inner pressure (Mpa)	Precession angle (deg)	Z- offset
R80	0.25	23	1

- The rubber layer's thickness is 3.5mm, and the metal sheet is 0.2mm in thickness.

• Z – offset is the displacement of the tool's nadir towards to the work piece

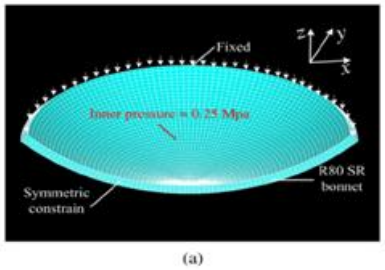

Fig 4.3(a): Model

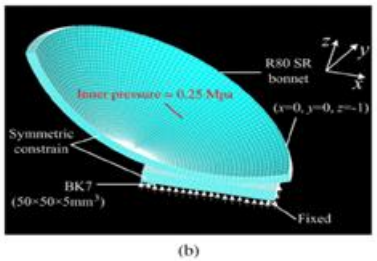

Fig 4.3(a): Model

4.1 MATERIALS & THEIR PROPERTIES

Table 4.1: material properties

Material	Density (kg/m^3)	Young's modulus (Mpa)	Poisson's ratio
Synthetic rubber	0.95E + 3	1.5	0.47
BK7	2.51E + 3	8.1E + 4	0.206
Stainless steel	7.30E + 3	1.9E + 5	0.26
Copper	8.96E + 3	1.1E + 5	0.35
Aluminum	2.70E + 3	6.8E + 4	0.36

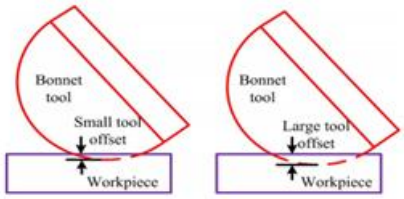

Fig 4.4: Schematic explanation about small and large tool offset

• TIF shape depends on the tool offset used in the polishing process. (Tool offset is the distance of the tool compressed to the work piece).

• Small tool offset is usually adopted in corrective polishing to generate Gaussian-like TIF.

• M-shaped TIFs induced by large tool offset are usually adopted in this stage to implement a higher material removal rate.

• Tool offset = 0.5mm , 1.6mm , 2mm

ISSN No: 2348-4845
International Journal & Magazine of Engineering, Technology, Management and Research
A Peer Reviewed Open Access International Journal

6. RESULTS

Mid-spatial frequency error suppression with high time-efficiency

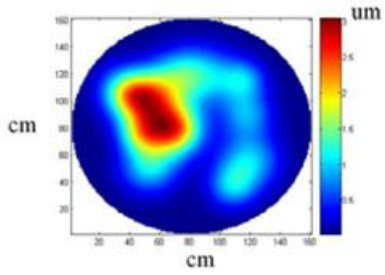

Fig 6.1: Target removal map

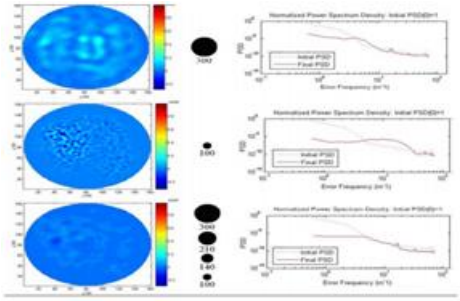

Fig 6.2: Shows the evolution of optical surface during the polishing process

Initial surface spec. (i.e. target error map spec.)			Final surface spec. (i.e. residual error map spec.)			Total polishing time (unit time $^{-1}$)
Surface error RMS (nm)	Slope error RMS (arcsec)	Error volume (cm^3)	Surface error RMS (nm)	Slope error RMS (arcsec)	Error volume (cm^3)	
701	0.522	1.31	36 *94.9%*	0.1 *80.8%*	0.072 *94.5%*	82
701	0.522	1.31	31 *95.6%*	0.277 *46.9%*	0.006 *99.5%*	774
701	0.522	1.31	10 *98.6%*	0.057 *89.1%*	0.005 *99.6%*	100

Percentile in italic represents the improvement ratio with respect to the initial surface specification for the surface error RMS, slope error RMS, and error volume. This is same as the figuring efficiency FE for the surface error RMS case.

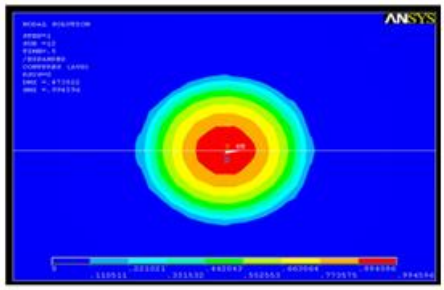

Fig 6.3: Simulation results of the contact pressure under different tool offset 0.5 mm

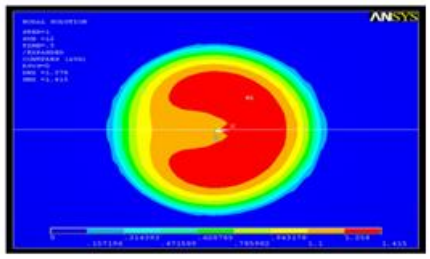

Fig 6.4: Simulation results of the contact pressure under different tool offset 1.6 mm

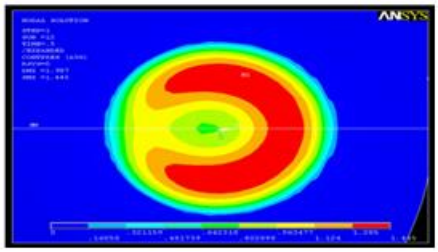

Fig 6.5: Simulation results of the contact pressure under different tool offset 2.0 mm

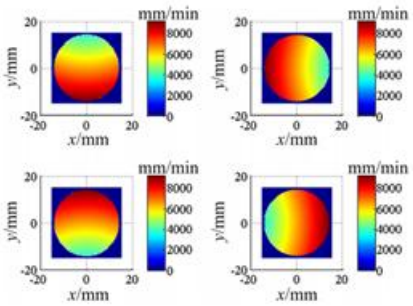

Fig 6.6: Velocity distribution in four directions (tool offset= 1.6 mm)

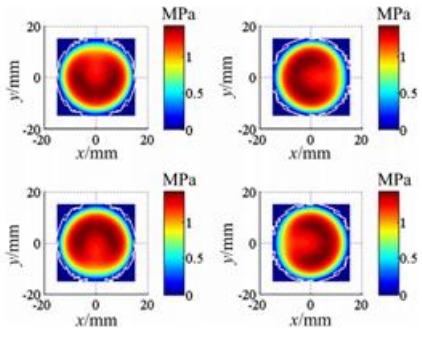

Fig 6.7: Contact pressure distribution in four directions

ISSN No: 2348-4845
International Journal & Magazine of Engineering, Technology, Management and Research
A Peer Reviewed Open Access International Journal

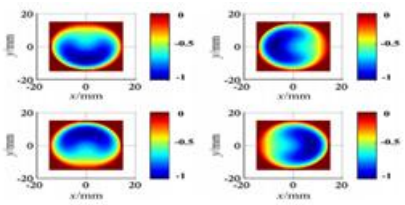

Fig 6.8: 4 Normalized TIF of tilted polishing in four directions

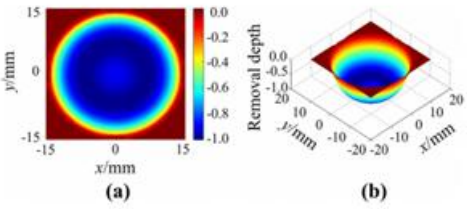

Fig 6.9: Normalized 4-discrete precession polishing TIF. a Top view, b isometric view

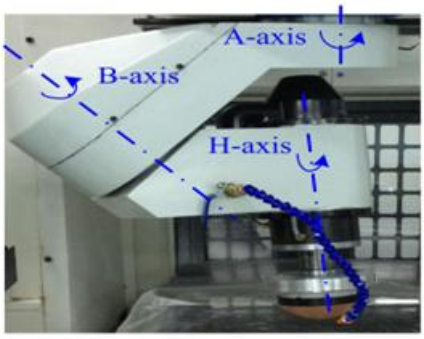

Figf 6.10: Experimental device

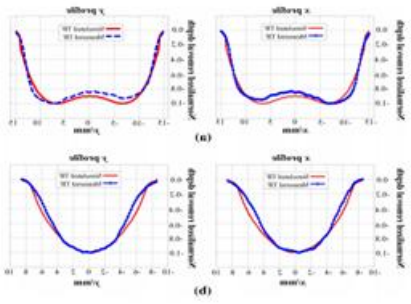

Fig 6.11: Comparison of the sectional profiles between simulated TIF and measured TIF. a TIF 1, b TIF 2

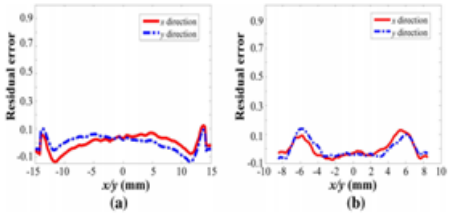

Fig 6.12: Residual error between the simulation TIFs and measured TIFs. a TIF 1, b TIF 2

CONCLUSION:

For BP, M-shaped TIF is as important as Gaussian-like TIF. ATIF model is presented based on the optimized finite element simulation model for contact pressure. The pressure distribution used in this model is generated directly based on the simulation result rather than fitting the simulated data using an equation. Hence, it can not only be used to model the M shaped TIF used in high-efficiency polishing stage but also can be used to model the Gaussian-like TIF. The verification experiments show that the simulated TIFs based on this modelare in good agreement with the actual measured TIF, which proves the effectiveness of this model.

8. REFERENCES:

[1] Gufran S Khan, Mikhail Gubarev, William Arnold and Brian Ramsey (2009), "Development of a Computer-Controlled Polishing Process for X-Ray Optics" SPIE 7437, pp. 1-12 2.

[2] H. Cheng (2014), "Independent Variables for Optical Surfacing Systems: Synthesis, Characterization and Application", Chapter 2- Tool influence Functions, DOI 10.1007/978-3-642-45355-7_2,

[3] Mamoru Mitsuishi, Kanji Ueda and Fumihiko Kimura (2008), "Manufacturing Systems and Technologies for the New Frontier", the 41st CIRP Conference on Manufacturing Systems, pp. 445

[4] C. Wang, Z. Wang, X. Yang, Z. Sun, Y. Peng, Y. Guo and Q. Xu (2014), "Modeling Of the Static Tool Influence Function of Bonnet Polishing Based On

ISSN No: 2348-4845
International Journal & Magazine of Engineering, Technology, Management and Research
A Peer Reviewed Open Access International Journal

FEA", International Journal of Advance Manufacturing Technology, Vol. 74, pp.341-349

[5] Preston, F. W (1927), "The Theory and Design of Plate Glass Polishing Machine", Journal of the Society of Glass Technology, Vol. 11, pp. 214-256

[6] LirongGuo and R. Shankar Subramanian (2004), "Mechanical Removal in CMP of Copper Using Alumina Abrasives", Journal of the Electrochemical Society, 151 (2) G104-G108

About Author's

Bylapudi Srinu
M.Tech (Machine Design) Student,
Department of Machanical Engineering,
Chaitanya Engineering College, Visakhapatnam.

P.Santhi
Assistant Professor,
Department of Machanical Engineering,
Chaitanya Engineering College, Visakhapatnam.